NTR&D
North Texas Research and Development Corporation

Post Office Box 5073
Denton, Texas 76203-5073

June 25, 1993

ONR CONTRACT N00014-93-C-0051
PROGRESS REPORT NO. 3 FOR MAY 16 - JUNE 15, 1993
ITEM NUMBER NRD0001AC - SHIPMENT NUMBER NRD0003

Additional substantial experimental progress has been made, in the third month of the project, in setting up equipment and testing for producing chaotic behavior with a CO_2 laser. The project goal is to synchronize and control chaos in CO_2 and other lasers, and thereby increase the power in ensembles of coupled laser sources. Numerous investigations into the chaos regime have been made, a second CO_2 laser has been brought on stream, work is progressing in the fourth month toward coupling the two lasers and control of the first laser. It is also intended to submit at least two papers to the Second Experimental Chaos Conference which is supported by the Office of Naval Research. Abstracts of those two papers are attached. Weekly Coordination Meetings of the project team continue to be held and are well attended. As the experimental work has progressed, two scheduling meetings are being held each week.

TECHNICAL EXPERIMENTAL PROGRESS:

Last month's report discussed the experimental investigation of nonlinear dynamics of CO_2 lasers which involved a new technique of inducing chaos. In this new technique, an acoustically modulated feedback of the laser light was used and led to chaotic dynamics at a very low modulation frequency of 375 Hz. Since then, new results have been obtained by an Electro-Optical Modulation (EOM) technique. In the new setup, the electro-optical modulator is placed in an external cavity outside the laser. This experimental arrangement does not require any rebuilding of the laser (all modulation schemes described by other authors used an EOM inside the laser cavity, and thereby necessitated significant modification of the laser). It also facilitates tuning of the laser and alignment of the EOM.

1. Experimental Setup

The current experimental setup is shown in Figure 1. This setup is the same as described in the previous progress report, except that the radio speaker is replaced by an EOM and a mirror (Ref. Figure 1 Items (4) and (5)). The EOM is driven by a power supply operating in the frequency range from 50 kHz to 150 kHz, and an amplitude range from 400 to 1600 V. In addition to the modulating amplitude, a DC bias of 1500 V is applied to the EOM. The entire setup is located on an optical table that is mounted on air legs to minimize mechanical vibrations. The laser signal from the laser grating is detected by a HgCdTe high frequency detector. The output signal of the detector is sent to a spectrum analyzer, after being amplified. The signal is also sent to the scope in the XY mode to record the phase portrait. The data thus obtained is digitized and transferred to a PC computer as follows:

> The time series data is obtained via a 10MHz, 8-bit, bipolar, two channel digitizer. Several series of data can be sampled at 1MHz, 2MHz, and 10MHz. The digitized data is then transferred to a 486DX50 PC via a Tecmar PC-Mate Lab Master interface card. Data is stored on the PC via a custom program written in C, in columns of 65535 data points. Phase portrait data is obtained by delaying the input to the first channel of the digitizer through a delay line, using the delayed signal as the input to the second channel of the digitizer. The same procedure is used for transference of the phase portraits. The spectrum is obtained using a HP 3585A 20Hz-40MHz Spectrum Analyzer. A Keithley Metrabyte IEEE 488 Interface board is used to transfer the data from the spectrum analyzer to the same PC. An additional custom

TEL: (817) 565-4990
TEL: (512) 834-8641
FAX: (817) 565-3802
1921 Edwards St., Suite 9, (Do not use for mail) Denton, Texas

program, written in C, is used to store the data. The spectrum analyzer's output consists of 1001 data points of frequency vs. dB. All data is then stored on tape for backup and archival purposes.

2. Results

Typical experimental results are shown in Figure 2. In the left column the frequency spectra are displayed, the middle column shows the respective time series, and finally, the right column contains the corresponding phase portraits (Intensity(t) vs Intensity($t+\tau$)). For this series of experiments the modulation frequency was kept constant at 83.00 kHz and the amplitude of the modulation signal was varied from 200 to 925 V. For a modulation amplitude of 200 V (Figure 2 a,b,c), the laser intensity simply follows the driving signal with a pronounced second and third harmonic present. As the modulation amplitude is varied (in this case increased) the laser output becomes more and more structured. Figure 2 d,e,f indicates period doubling (2T) which occurs at a modulation amplitude of 250 V. Subsequently, periods 4 and 8 are obtained for modulation amplitudes of 400 and 500 V, respectively, as shown in Figure 2 g,h,i and 2 j,k,l.

Finally, at a modulation amplitude of 925 V, the frequency spectrum of the laser output changes into a broadband spectrum with a rise in the floor level. This is a definitive indication that the system is driven into chaos, as shown in Figure 2 m. The chaotic attractor (Figure 2 O) has a characteristic shape typical for chaotic states obtained at other driving frequencies. The complete state diagram of the CO_2 laser in frequency - amplitude space (F=driving frequency, A=driving amplitude) is shown in Figure 3. It indicates that there is a continuous frequency interval for which laser output can become chaotic. This result is new, as the previously reported chaotic states were obtained for driving frequency equal to the frequency of the relaxation oscillations of the CO_2 laser.

Initial attempts to optically couple two lasers were made and appear successful. These initial results were obtained on the last day of this project period. Coupling induced instabilities were observed in the system. Figures 4 and 5 show phase portraits and frequency spectra for the instabilities in the coupled laser system. The phase portraits are similar to those observed for the single chaotic laser. The corresponding frequency spectra, shown in Figures 5 b and 5 c, show discrete frequencies in addition to broadband noise.

TECHNICAL THEORETICAL PROGRESS:

The capture of experimental data, in a digital format, has permitted theoretical analysis of the data to proceed. The analytical and theoretical simulation results are discussed in the attached, 12 page, Appendix A.

SUMMARY:

* A new EOM technique has been used to investigate instabilities and chaos in CO_2 gas lasers.
* The new technique uses an external electro-optically modulated feedback of the laser beam.
* A complicated sequence of interlocking periodic and chaotic regimes in the frequency range of 50 kHz to 85 kHz has been observed.
* A state diagram of the system, in the parameter space of the EOM, has been obtained.
* Theoretical analysis of the data shows the chaos regime has been determined and documented with the laboratory equipment, techniques, and data acquisition system.
* Lasers were coupled and instabilities in coupled lasers were observed.

END

DTIC QUALITY INSPECTED 8

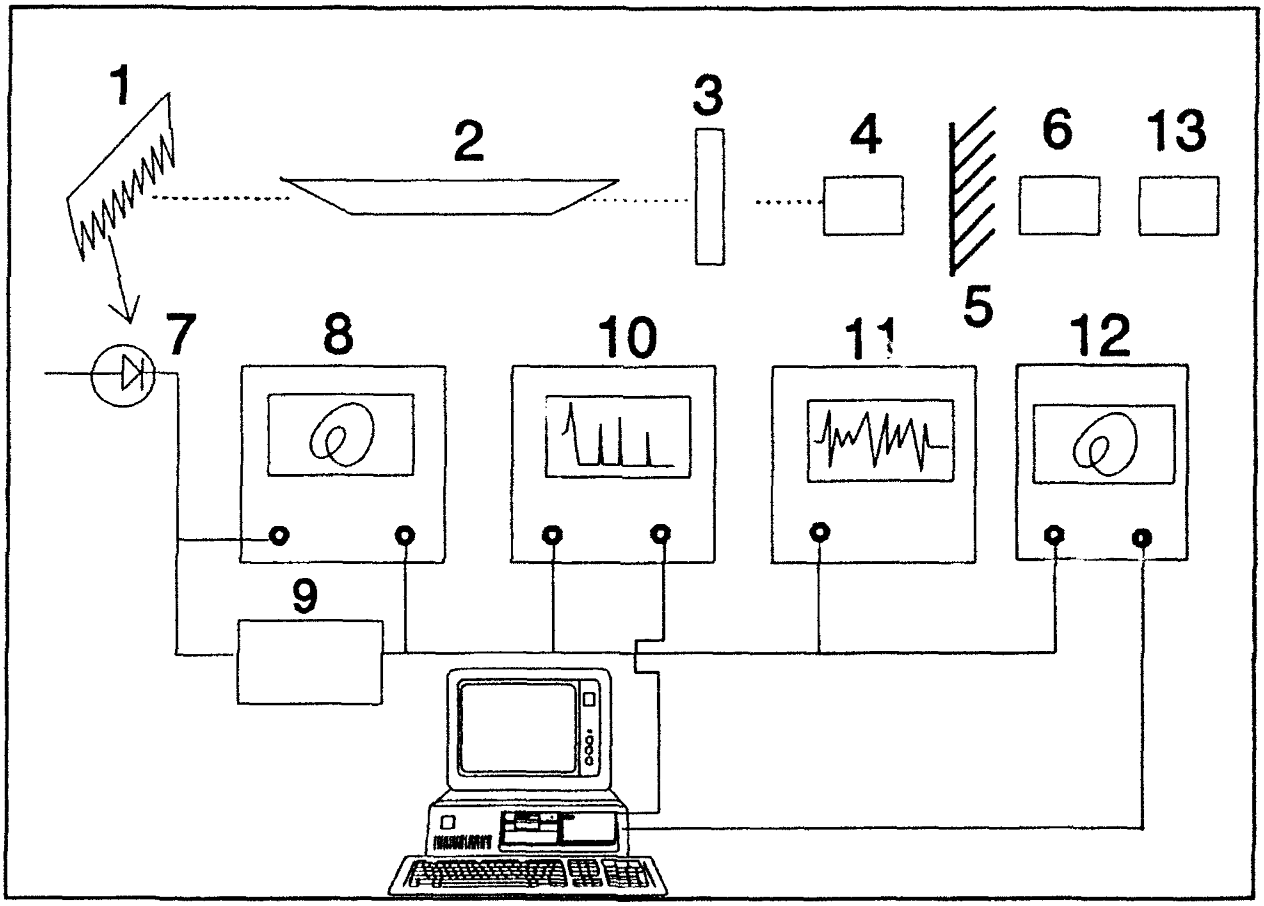

Figure 1: Experimental set up: 1. grating 2. CO_2 laser tube 3. output mirror 4. EOM 5. mirror 6. frequency generator 7. LN_2 cooled HgCdTe detector 8. oscilloscope 9. delay line 10. spectrum analyzer 11. oscilloscope 12. digitizer 13. DC power supply 14. PC computer

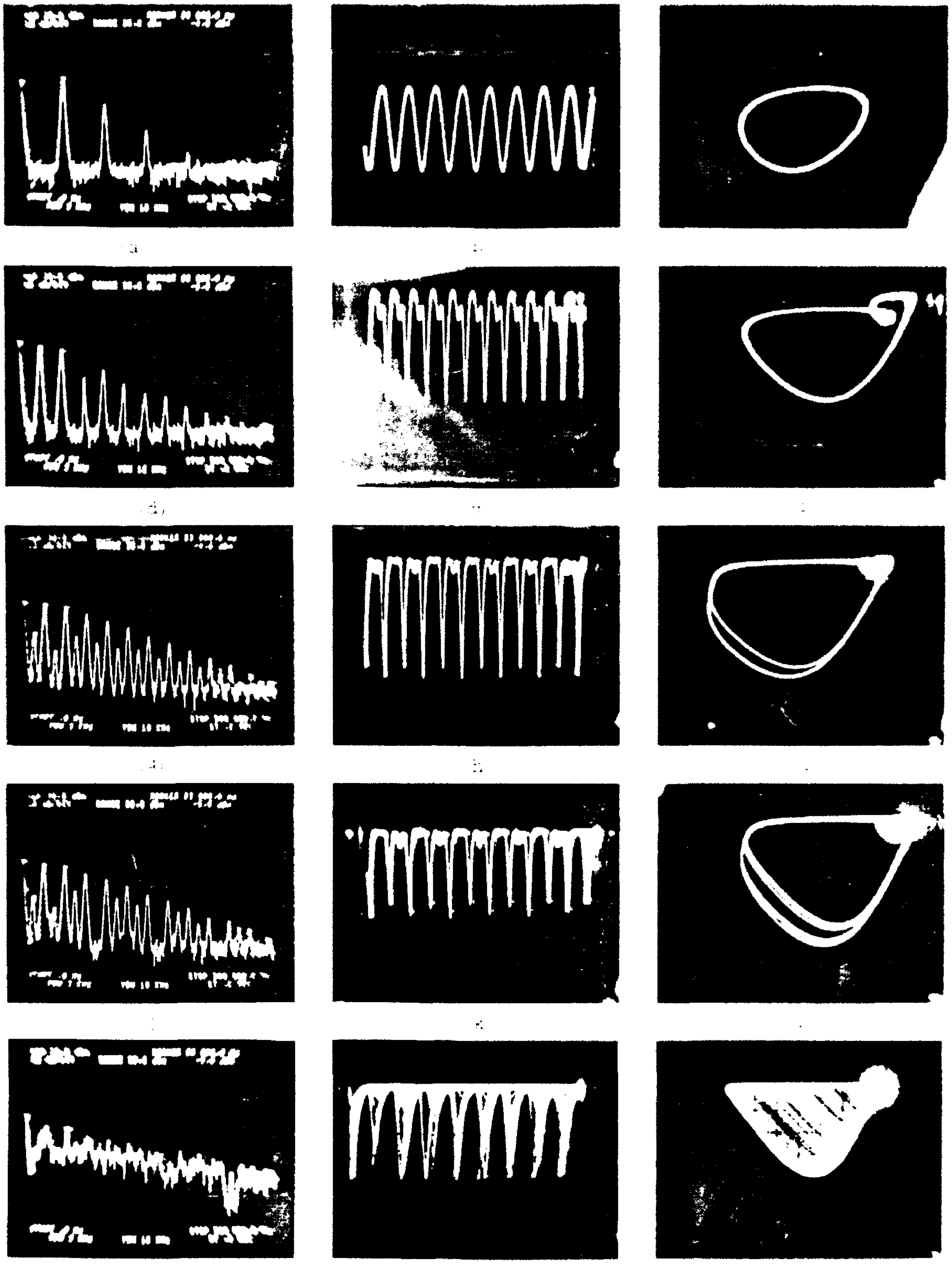

Figure 2

CO_2 Laser Generated Data

Left column - frequency spectra,
Center column - time series,
Right column - phase portraits.

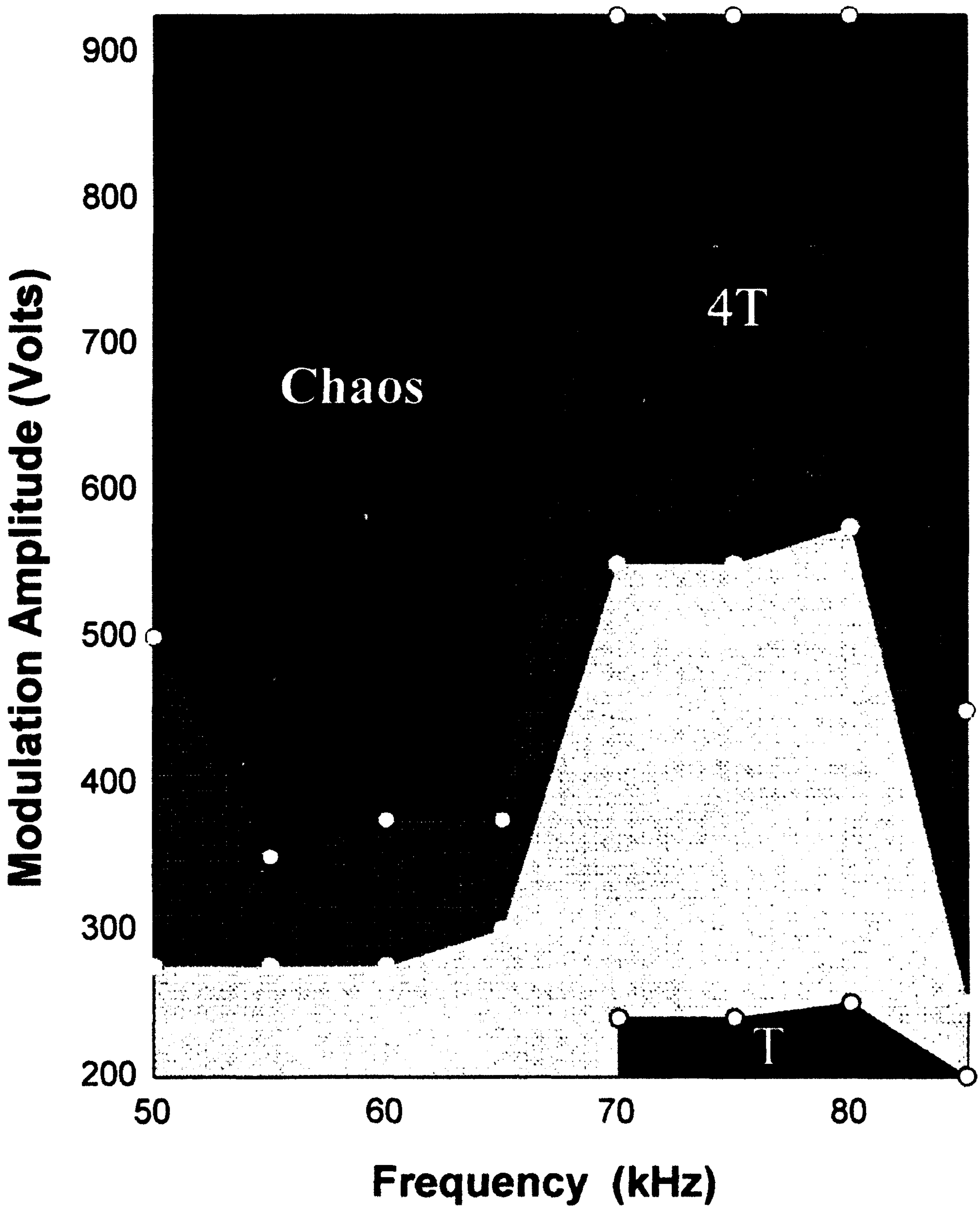
Chaos
4T
T
Modulation Amplitude (Volts)
900
800
700
600
500
400
300
200
50
60
70
80
Frequency (kHz)

Figure 3

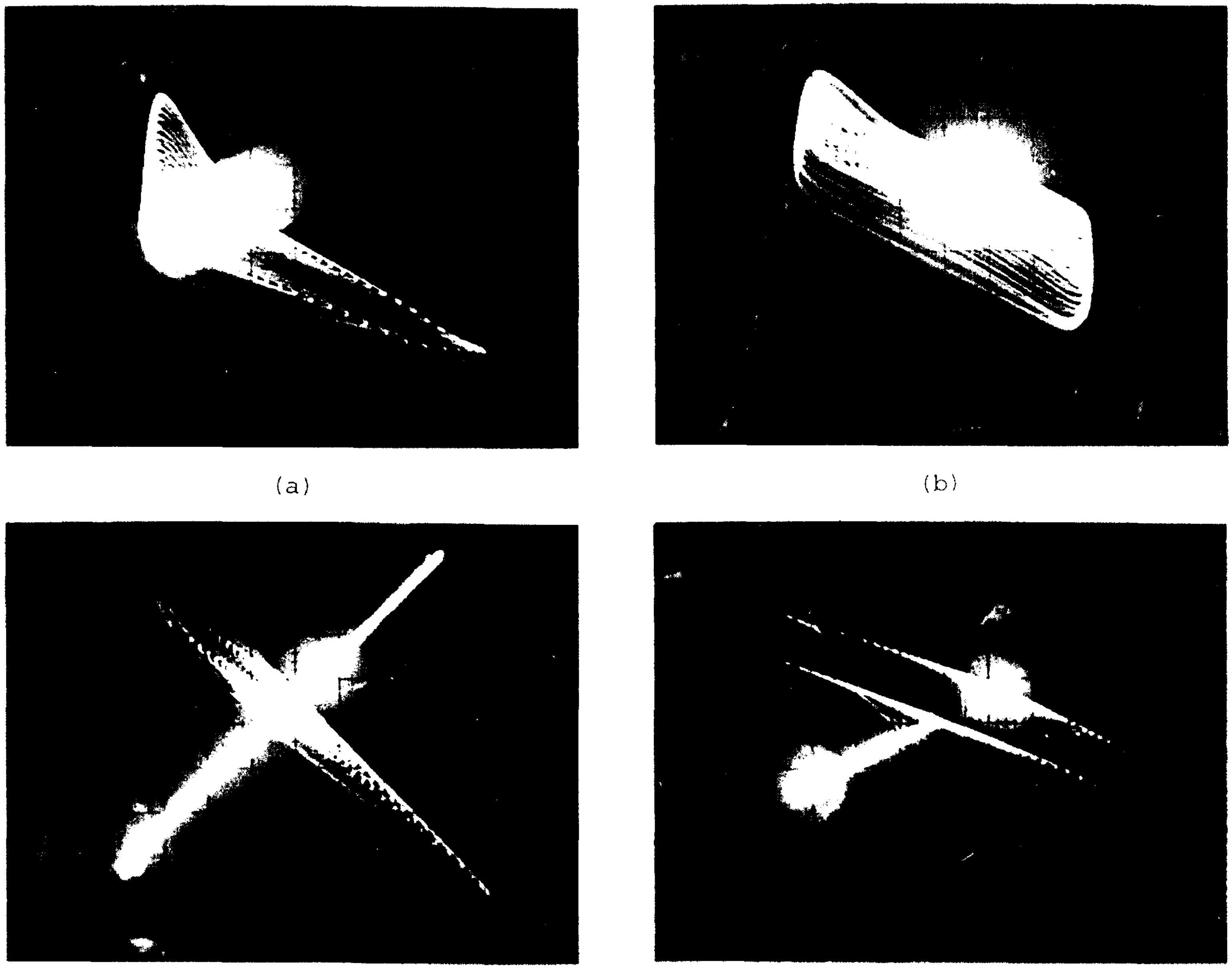

Figure 4
Instabilities In Coupled Lasers

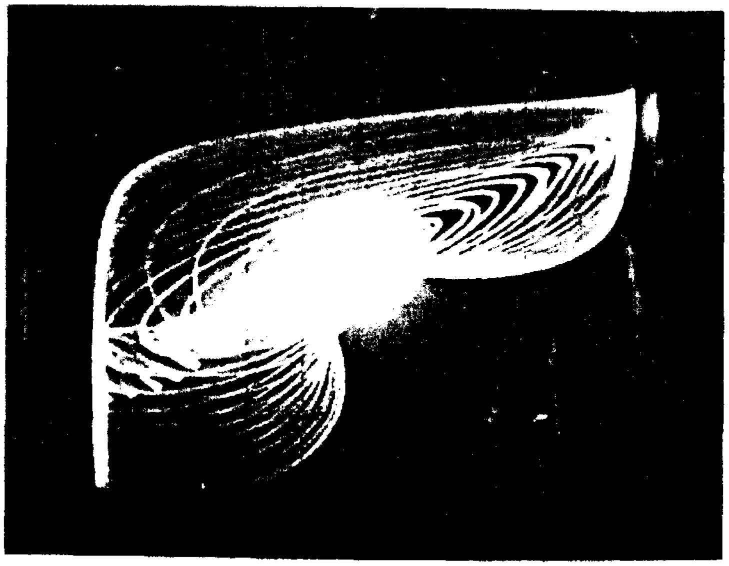

(a)

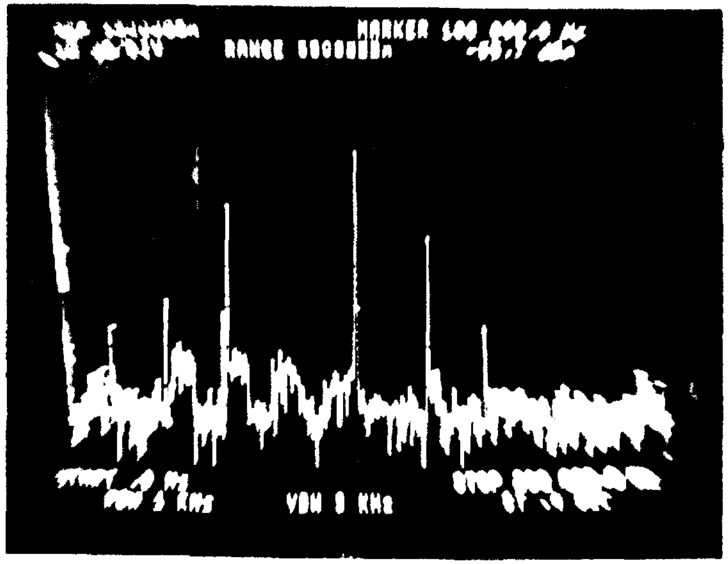

(b)

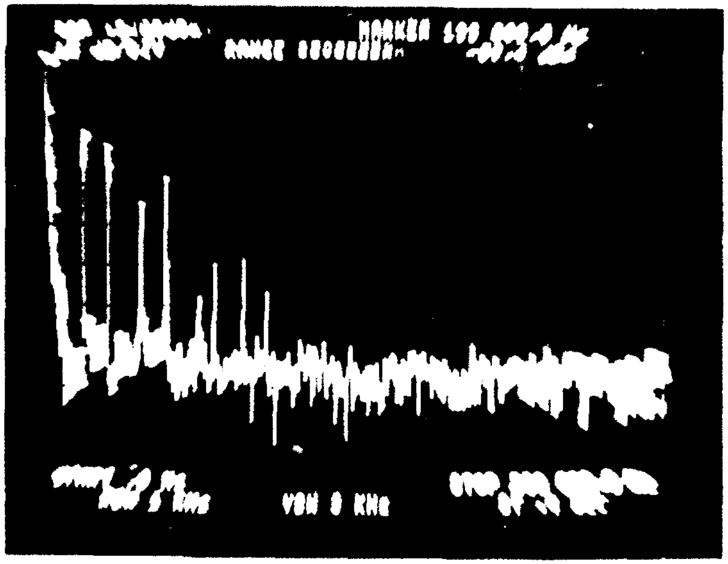

(c)

Figure 5
Instabilities in Coupled Lasers

Multistability and chaos in a CO_2 laser with externally modulated optical feedback *

J. Prasad[b], E.M.Rabinovich[b], J.M. Perez[a,b], C.L. Littler[a], J.M. Kowalski[a], B.J.West[a]

[a]Department of Physics, University of North Texas, Denton, TX 76203; [b]North Texas Research and Development Corp., P.O.Box 5073, Denton, TX 76203.

As in the case of semiconductor lasers, the class B CO_2 lasers show an extreme sensitivity to an optical feedback from external mirrors, rough reflecting surfaces and external cavities with modulated characteristics. We report on laser instabilities caused by an electro-optical modulation in the external cavity, by a fed-back radiation reflected from an external moving surface, and by a fed-back beam modulated by an acoustic wave pasing through the external cavity. Experimental results show the presence of stable multiple limit cycles, random attractor switching, and "hard" transition to chaos, in addition to more standard transition scenarios . The time series data for chaotic and "noisy periodic" orbits are examined, and the applicability of the proposed dynamical equations for these feedback schemes is discussed.

Control of Chaos in a CO_2 Laser *

J.M. Perez[a,b], E. Rabinovich[b], J. Prasad[b], C.L. Littler[a], R.E. Stallcup[a], J. Steinshnider[a], and A.F. Aviles[a], [a]Department of Physics, University of North Texas, Denton, TX, 76203; [b]North Texas Research and Development Corporation, P.O. Box 5073, Denton, TX, 76203.

We have experimentally controlled chaos in a CO_2 laser. The CO_2 laser was driven into a chaotic state by injecting a feedback beam modulated by an electro-optical modulator. The driving frequency of the electro-optical modulator was varied from 50 kHz to 85 kHz, which includes the estimated frequency of relaxation oscillations of the CO_2 laser close to the excitation threshold. For a given frequency in this range, period doubling bifurcations, intermittency and chaos were observed as a function of the voltage applied to the modulator. The chaotic states were successfully controlled using a modified proportional feedback technique. The controlling pulses were applied to the modulator and were less than 2% of the modulation voltage. Chaos was controlled to period 2 and period 1 orbits. Preliminary applications of these techniques to control of chaos in coupled CO_2 lasers will also be discussed.

* Work supported by the Office of Naval Research through Contract Number N00014-93-C-0051 with North Texas Research and Development Corporation.

Appendix A

DYNAMICS OF A CO_2 LASER WITH AN EXTERNALLY MODULATED FEEDBACK- THEORY AND SIMULATIONS

I.THE APPLICABILITY OF A MODEL WITH MODULATED LOSSES

CO_2 lasers belong to a class of lasers characterized by the polarization varaiable having very short relaxation time $\gamma_{\perp}^{-1}$. This relaxation time is approximately three orders of magnitude shorter than the relaxation time k^{-1} of the electric field. The longest time scale in this hierarchy is the relaxation time $\gamma_{\parallel}^{-1}$ of the population inversion, where typically $k >> \gamma_{\parallel}$. In this region of parameter space of the simplest rate equations for the light intensity $I \geq 0$ and the population inversion N variables are:

$$\dot{I} = -kI + \alpha IN,$$
$$\dot{N} = -\gamma_{\parallel}(N - N_0) - 2\alpha IN, \qquad (1)$$

where α is the Einstein coefficient and N_0 is the unsaturated value of the inversion variable. The system (1) is easily obtained from the semiclassical laser equations assuming fast relaxation of polarization, and restricting the considerations to a single mode. However, Eqs. (1) can also be considered as a reasonable first order approximation to a multimode case, where the modes are only weakly coupled, the intensities of one part of the modes decay to zero after their excitation, and the remaining modes have close decay rates and gain coefficients. In our case, when a part of the emitted radiation is intensity-modulated in an external cavity and then returned to the laser cavity, the model (1) is a reasonable approximation provided that $k(t)$ is an effective, time-dependent coefficient: $-kI -> -kI + (k_f - \varepsilon f(t))I -> -k(1 + \varepsilon f(t))I$ where $(k_f - \varepsilon f(t))I$ is the modulated feedback term.

The qualititative analysis of the 2-D system (1) with polynomial nonlinearities is a rather straightforward exercise, and, for the reader's convenience we repeat it here.

If a state space of a laser system includes the intensity variable, then it has to be restricted by the obvious condition $I \geq 0$. For the system (1) all trajectories initiated in the half-plane $I \geq 0$ indeed remain there forever, as the vector field governing the system does not have non-zero transverse components on the N axis. Additionally, it is clear that the positive and negative parts of the N axis are themselves invariant and both belong to the stable manifold of the equilibrium point ($I = 0$, $N = N_0$). The equilibrium ($I = 0$, $N = N_0$) is a sink for $N_0 < k / \alpha$.

For $N_0 > k/\alpha$ there is an additional equilibrium point

$$(I_{eq} = (\gamma_{\parallel}/2\alpha)(N_0 - N_{eq})/N_{eq}, N_{eq} = k/\alpha)$$

which corresponds to a globally stable lasing state, as we show below using a different representation of the system dynamics. For N_0 close to k/α the lasing equlibrium is initially a sink, which is replaced by a stable focus for $N_0 > N_1$. Here N_1 is the threshold value of N_0 above which the eigenvalues of the linearization operator at the lasing equilibrium have non-zero imaginary parts. In our parameter regime N_1 is very close to N_0. For $N_0 > N_1$ the lasing state is then asymptotically approached from any initial conditions with damped oscillations of characteristic frequency $\omega_r(N_0)$ called the ringing frequency of the laser. Obviously, $\omega_r(N_0) \to 0$ for $N_o \to N_1$ from above.

The system (1) undergoes an interesting and highly non-trivial modification under the conditions of an external drive, as it often happens for any driven relaxational oscillator. Several different driving schemes of a CO_2 have been considered in literature.

Below we will concentrate on previously mentioned systems with modulated losses,

$$\dot{I} = -k(1 + \varepsilon f(t))I + \alpha IN,$$
$$\dot{N} = -\gamma_{\parallel}(N - N_0) - 2\alpha IN, \quad (2)$$

where ε is a small parameter and $f(t)$ is a periodic function of some characteristic period $2\pi/\Omega$. Equations (2) could be replaced by an autonomous system in an usual way by considering time as a dynamical state variable ($\dot{t} = 1$). The resulting flow does not contract the volume everywhere. However , in the physical halfspace (I>0) and for $N_0 > k/\alpha$ one can use a *nonlinear* transformation to new variables

$$u = \ln(I/I_{eq}), \quad v = (N - N_{eq})/N_{eq} \quad (3)$$

and describe the dynamics by the following autonomous system

$$\frac{du}{d\tau}=\frac{k}{\omega_r}(v-\varepsilon f(t)),$$
$$\frac{dv}{d\tau}=-\frac{\gamma_{\parallel}}{\omega_r}[v-v_0+v_0(v+1)e^u],$$
$$\frac{dt}{d\tau}=\omega_r^{-1}$$

(4)

where we work with the dimensionless time $\tau=\omega_r t$, and $v_0=(N_0-N_{eq})/N_{eq}$. The system (4) is volume-contracting in the whole state space and it is a convenient starting point for numerical and analytical studies.

Following [1] it is instructive to replace the system (4) by an equivalent second-order ODE. In the special case of harmonically modulated losses

$$f(t)=\cos\frac{\Omega}{\omega_r}\tau=\cos\overline{\Omega}\tau, \tag{5}$$

the resulting equation has the form

$$\frac{d^2u}{d\tau^2}-1+e^u=-\omega_r(\lambda_1 e^u+\lambda_2)\frac{du}{d\tau}-\varepsilon(e^u+v_o^{-1})\cos\overline{\Omega}\tau+\frac{\varepsilon\,\overline{\Omega}\omega_0}{\gamma_{\parallel}v_0}\sin\overline{\Omega}\tau, \tag{6}$$

where $\lambda_1=k^{-1}$, $\lambda_2=v_0^{-1}\lambda_1$ are two additional small parameters of the system. Thus one arrives at a physical picture of a Hamiltonian system

$$\frac{d^2u}{d\tau^2}-1+e^u=0 \tag{7}$$

(a particle of unit mass in the potential well $V(u)=-u+e^u$) perturbed by a small , nonlinear friction term, and a small effective "driving term"

$$\varepsilon A(u)\sin(\overline{\Omega}\tau-\delta(u)) \tag{8}$$

with a u- dependent amplitude and phase:

$$A(u)=[(e^u+v_0^{-1})^2+(\overline{\Omega}\omega_r/\gamma_{\parallel}v_o)^2]^{1/2}\ ,\quad \tan\delta(u)=\gamma_{\parallel}v_0(e^u+v_0^{-1})/\overline{\Omega}\omega_r. \tag{9}$$

After introducing the "momentum" variable $p=du/d\tau$, the Eq.(6) can be replaced by yet another system of first order ODE's, which is the most convenient one for numerical integrations. The friction term in Eq.(6), although small, ensures the global stability of the lasing equilibrium of an autonomous laser ($\varepsilon = 0$). Indeed, $L(u,p) = (1/2)p^2 + e^u - u$ is a Lyapunov function of the system, stricly decreasing along all trajectories originating away from the equilibrium. Consequently, limit cycles are impossible for the undriven system (this conclusion can also be reached after a direct analysis of the vector field governing the original system (1)).

In the driven case one can use the same Lyapunov function to show that closed trajectories are not allowed in a region in the (u,p) space given by

$$|p| > \frac{\varepsilon A(u)}{(\lambda_1 e^u + \lambda_2)\omega_r} . \tag{10}$$

The dynamics of the driven system (6), as should be expected is considerably richer than the autonomous case and only limited analytical results are available here.

We are testing the applicability of the modulated losses model to the problem considered, and we are carrying out respective numerical simulations. In particular, more attention is being paid to the multistability problem and to the construction of a reasonably complete phase diagram in the parameter space (driving frequency, driving amplitude). We review existing theoretical literature on the model (see the references below), correct some errors and discrepances therein, and add some new results (stability regions, Lyapunov first method, calculation of the Lyapunov spectra).

As an illustration, we attach an example of a "hard" transition to chaos found in numerical simulations (Fig.1-). On all these figures "the x-axis" stands for the dimensionless time τ axis, and "the y-axis " correspond to the u variable (logarithm of normalized intensity). The reduced driving frequency was set constant, $\overline{\Omega}=2$. All simulations were run for the same set of initial conditions for the (u,v) variables: u(0)=0.1, v(0)=0.2 and with v_0=0.1.For the amplitude $\varepsilon = 10^{-4}$ of the driving signal, the laser is driven into a periodic orbit (Fig.1).This type of behavior persists up to the amplitude $\varepsilon=2\times10^{-2}$, where the laser enters the chaotic state (Fig.2). The chaotic state persists for amplitudes up to $\varepsilon=1.0$ (Fig.3, $\varepsilon=4\times10^{-2}$, Fig.4, $\varepsilon=6\times10^{-2}$, Fig. 5, $\varepsilon=0.50$, Fig.6, $\varepsilon=1.0$). For larger values of the amplitude, the chaotic state has very interesting features. It can be described as a slowly drifting, and then abruptly changing periodic state (comp. Fig.7 when for $\varepsilon=1.0$, the system has been monitored for an interval four times longer than in all previous cases). Such behavior, often observed in the feedback experiment, is typically explained as caused by technical instabilities of the laser. The enclosed simulations demonstrate that the described behavior may also be explained in terms of the principally simple deterministic model.

LITERATURE

1. Matorin, I.I., A.S. Pikovski,and Ya. I. Khanin, Multistability and autostochasticity in a laser with a delayed-response active medium subjected to periodic loss modulation, Sov. J. Quantum Electron. **14**, 1401-1405 (1984). (R)

2.Schwartz, I.B., Sequential Horseshoe Formation in the Birth and Death of Chaotic Attractors, Phys.Rev.Lett., **60**, 1359-1362 (1988).

3.Schwartz, I.B., Infinite primary saddle-node bifurcation in periodically forced systems, Phys.Lett. **126**, 411-418, 1988.

4. Dangoisse, D., P. Glorieux, and D. Hennequin, Phys. Rev. Lett. **57**, 2657-60 (1986).

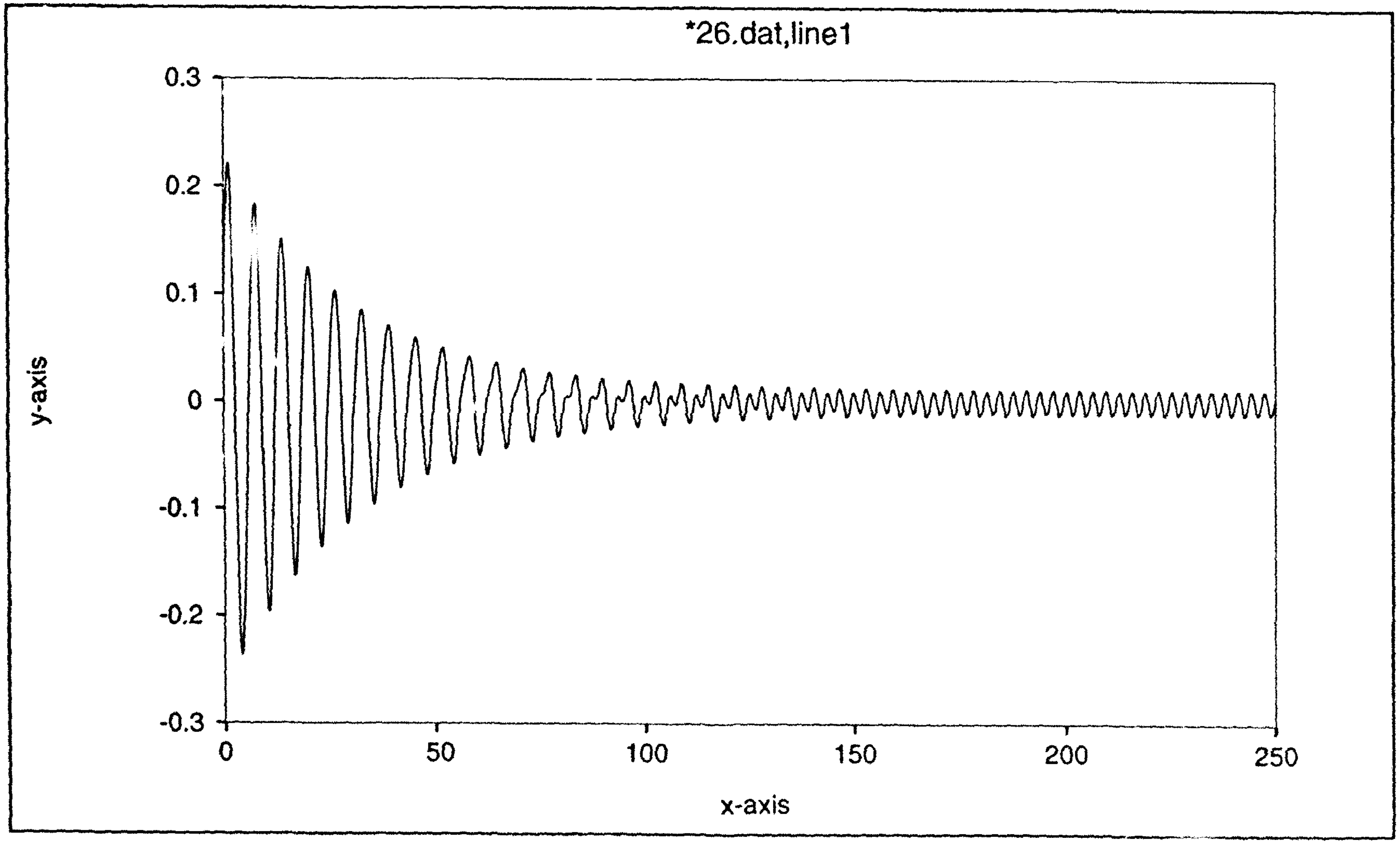

FIG. 1

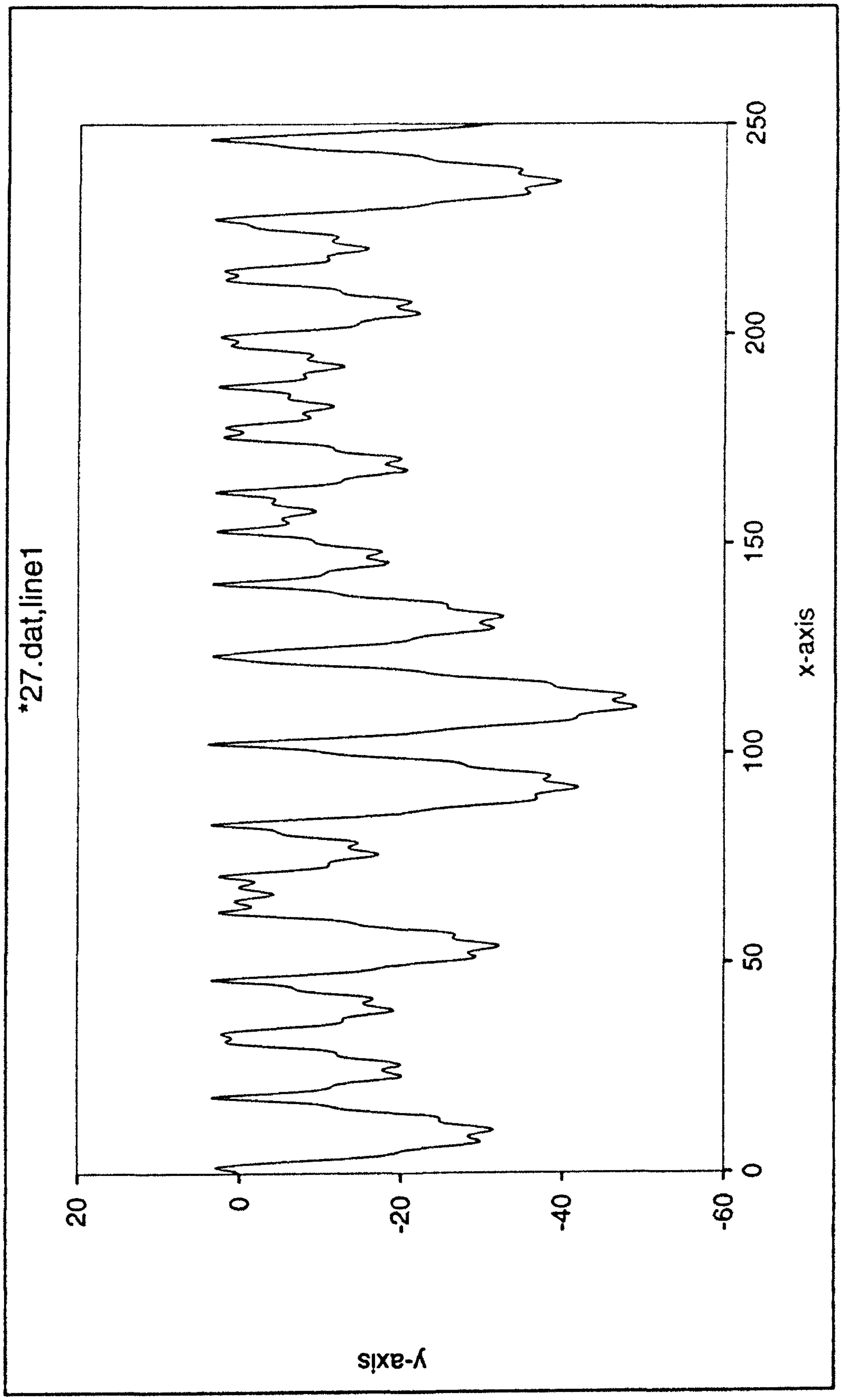

FIG. 2

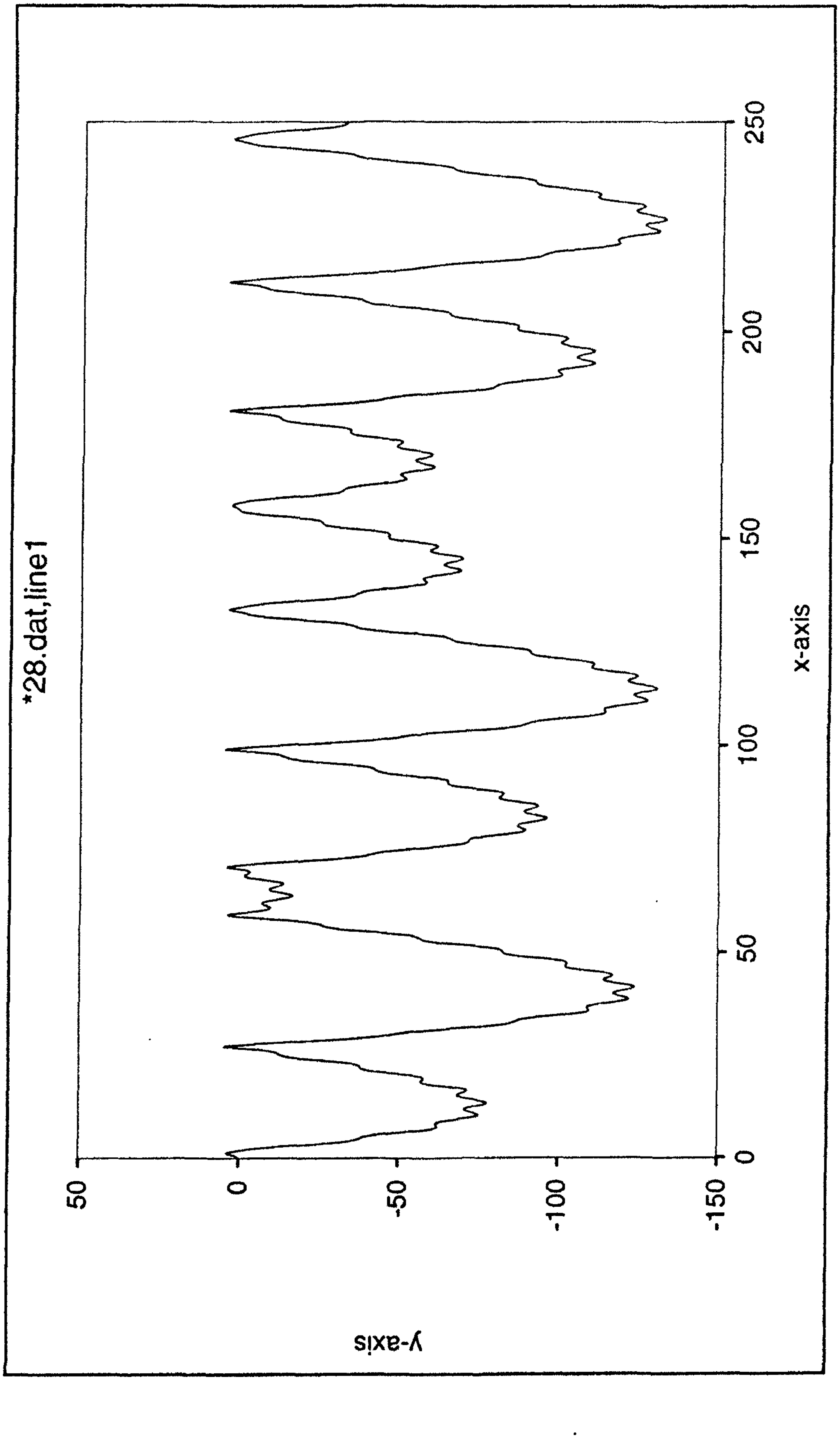

FIG. 3

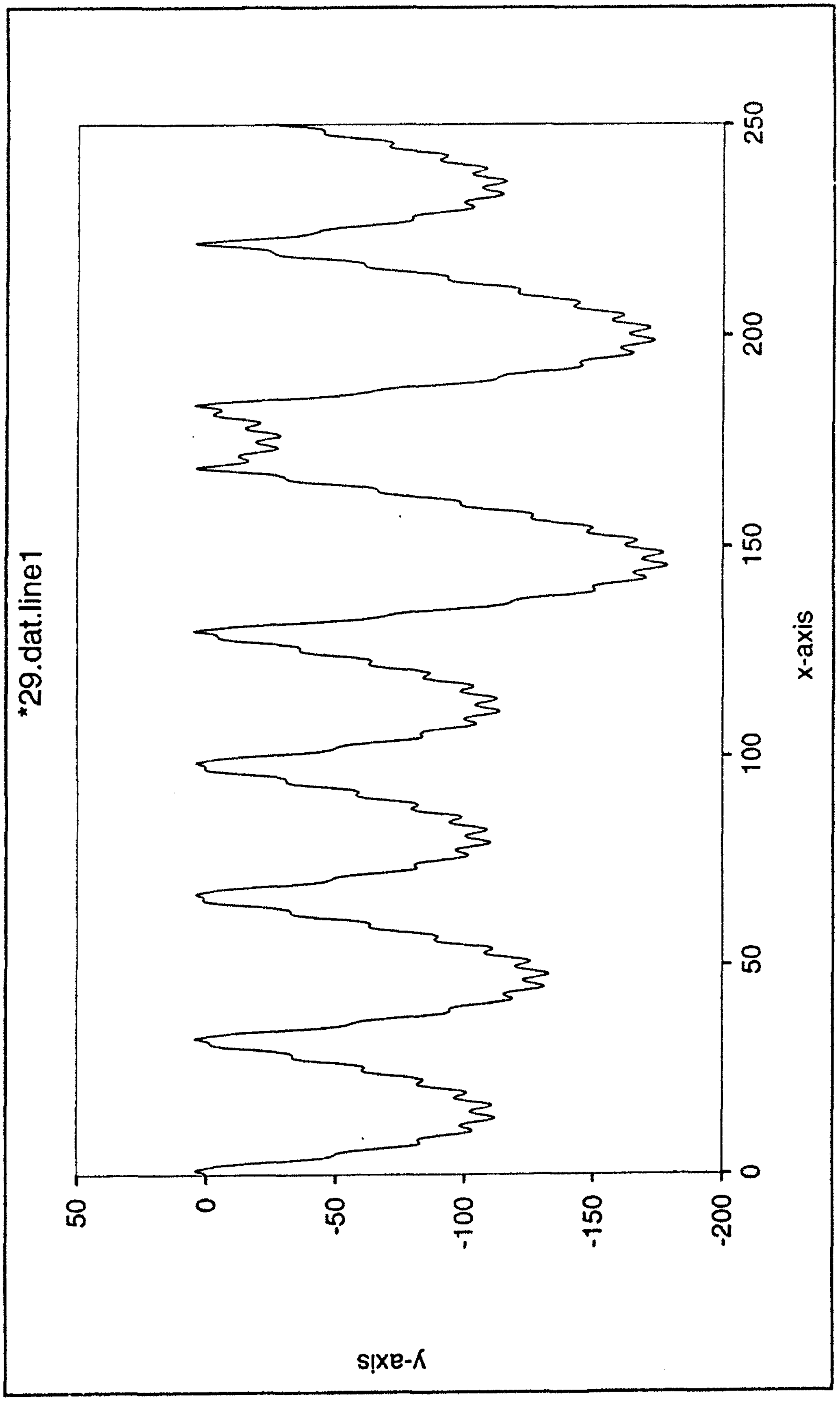

FIG. 4

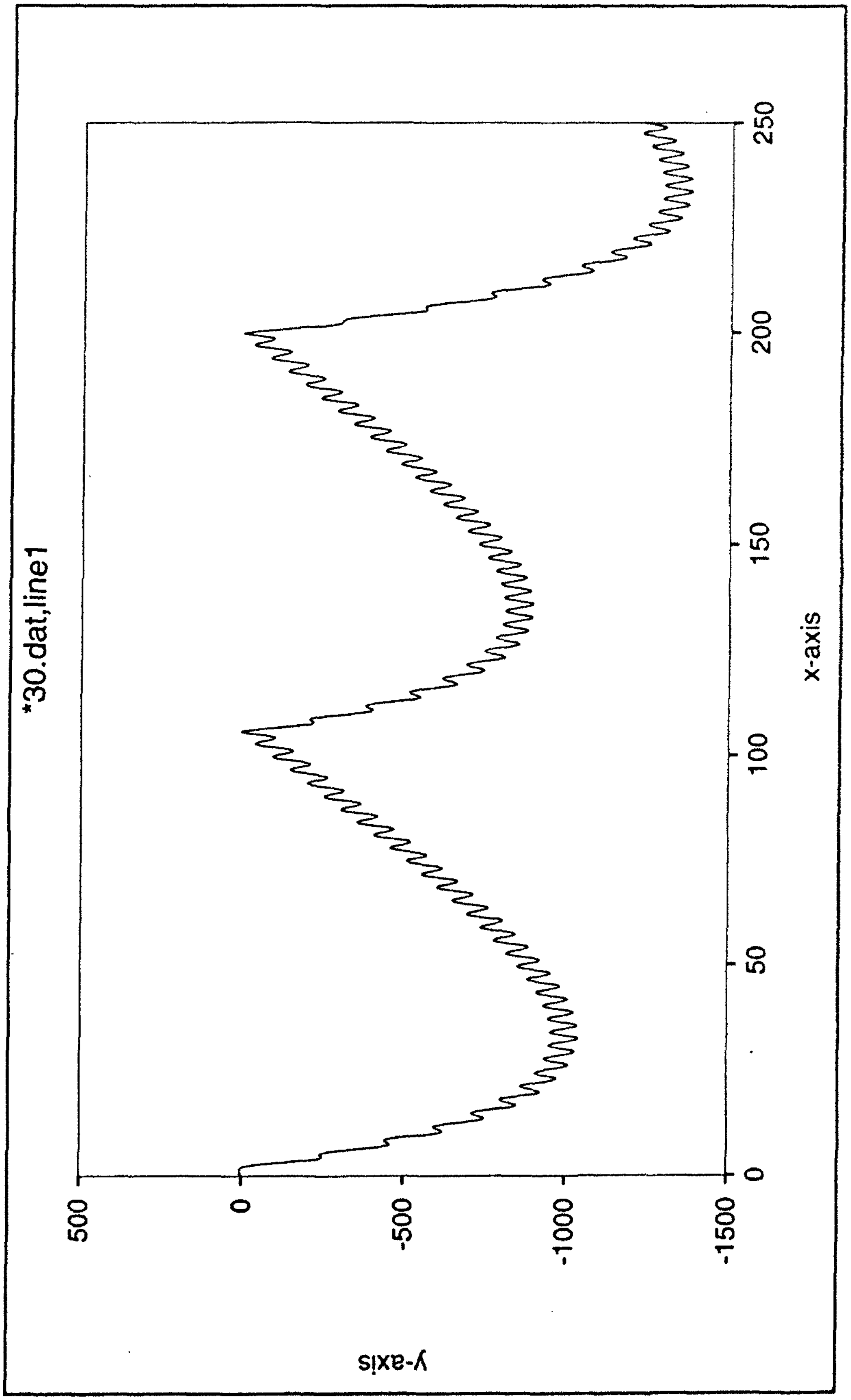
*30.dat,line1
y-axis
500
0
-500
-1000
-1500
x-axis
0
50
100
150
200
250

FIG. 5

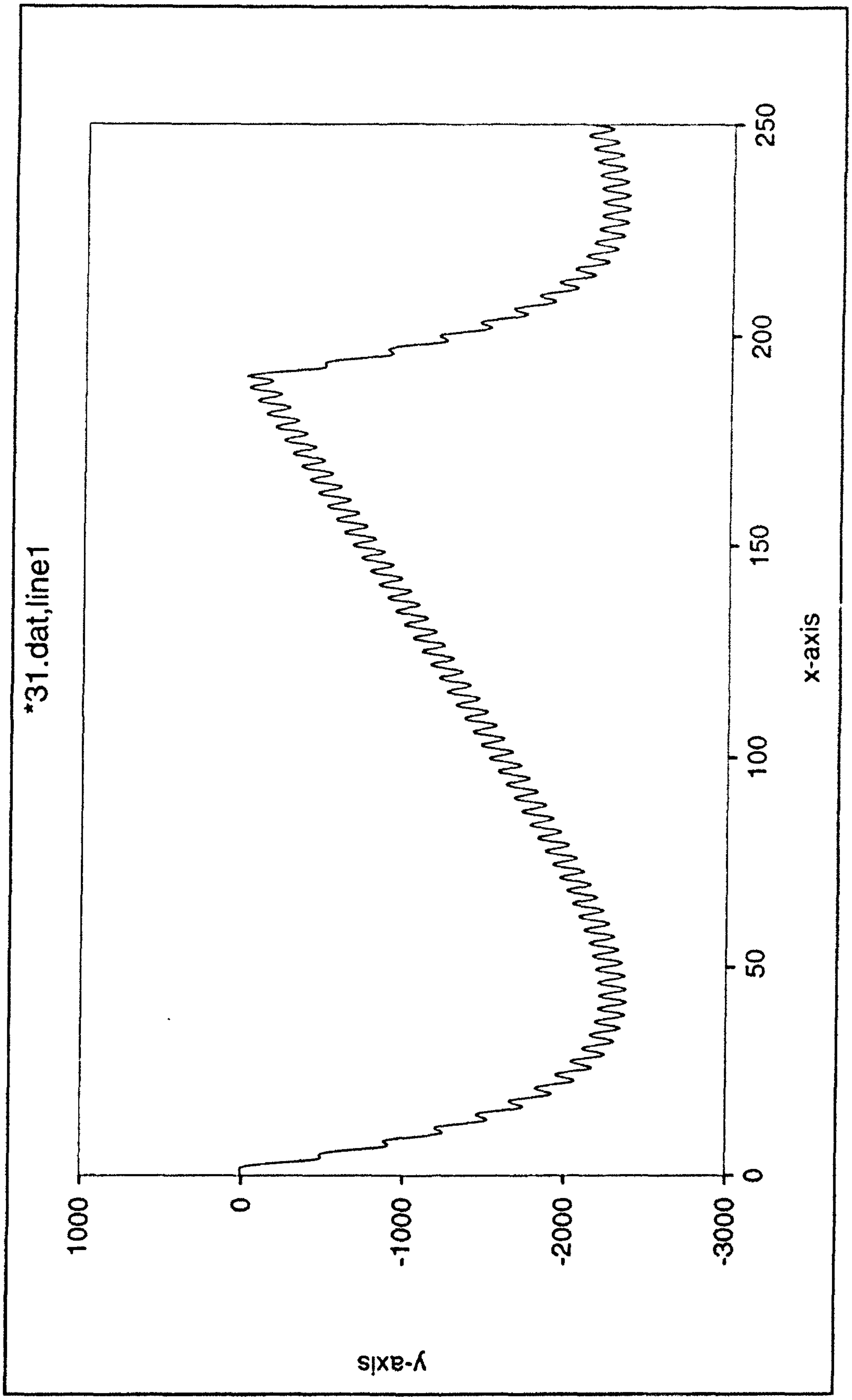
*31.dat,line1
y-axis
1000
0
-1000
-2000
-3000
x-axis
0
50
100
150
200
250

FIG. 6

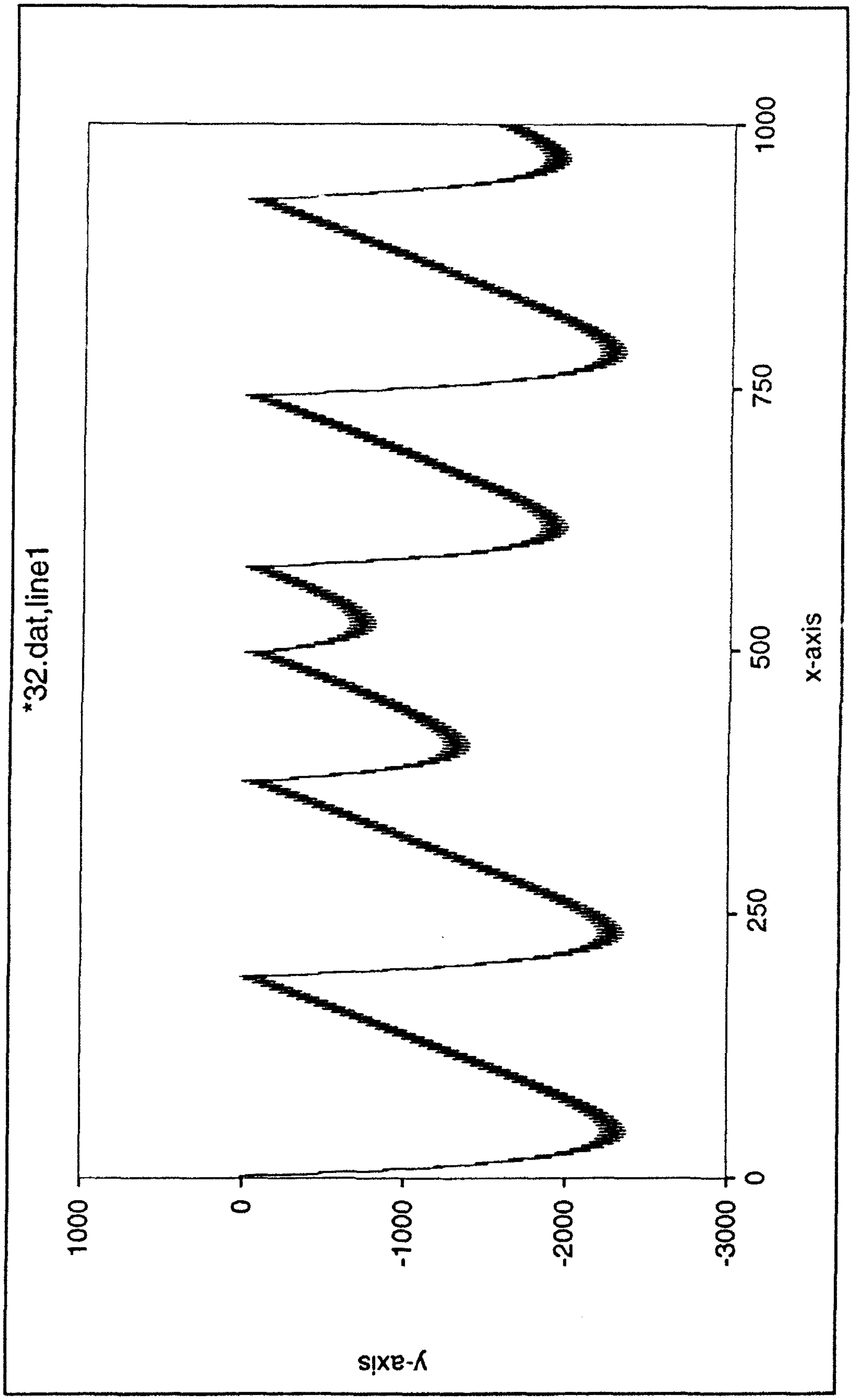
*32.dat,line1
y-axis
1000
0
-1000
-2000
-3000
x-axis
0
250
500
750
1000

FIG 7